JCTC Journal of Chemical Theory and Computation

Analyzing the Selectivity and Successiveness of a Two-Electron Capture on a Multiply Disulfide-Linked Protein

Élise Dumont,*,† Adèle D. Laurent,‡ Pierre-François Loos,§,‡ and Xavier Assfeld‡

Laboratoire de Chimie, UMR 5182 CNRS École Normale Supérieure de Lyon, 46, allée d'Italie, 69364 Lyon Cedex 07, France, and Équipe de Chimie et Biochimie Théoriques, UMR 7565 CNRS-UHP, Institut Jean Barriol (FR CNRS 2843), Faculté des Sciences et Techniques, Nancy-Université, B.P. 70239, 54506 Vandoeuvre-lès-Nancy, France

Received February 23, 2009

Abstract: Hybrid QM/MM calculations were performed on a circular macropeptide (kalata B1, PDB ID 1NB1) containing three disulfide linkages, to evaluate their respective reactivities toward (gas-phase) electron valence-attachment of one and two electron(s). The three disulfide bonds -CH_2-S-S-CH_2- were simultaneously described at the MP2/6-31+G**(S),6-31G*(C,H) level of theory, and the remaining of the 29 residues of kalata B1 were described by the CHARMM27 force field. The one-electron addition is favored on the linkage between cysteine residues 1 and 15, Cys(1−15), by ca. 1 eV over the two other disulfide linkages. The decomposition of the overall effect into geometrical and electrostatic contributions evidence (i) the key role of an arginine (R24) and (ii) a weaker geometrical penalty for elongating the nonstructural Cys(1−15) linkage. The addition of a second electron leads to the formation of the dithiolate Cys(1,15), favored by more than 1 eV over other adducts (either dithiolates or diradical dianionic species). This can be traced back to a structural reorganization, with a flip of R24 side chain. Its positively charged extremity points almost equidistantly toward one thiolate -CH_2-S^-, hence stabilizing this dianion.

I. Introduction

The existence of three-electron two-center (2c-3e) bonds has been postulated by Pauling[1] as early as 1931. An elegant theory was derived five decades later for predicting the relative stability of such hemibonded species[2] and was closely related to experimental data.[3] Their stability has been proved by a wide range of technics (pulse radiolysis,[4−6] electron spin resonance,[7] laser flash photolysis,[4] electrochemistry),[8] with a typical dissociation energy (ca. 20−30 kcal/mol) allowing a proper observation.

A strong motivation for the study of 2c-3e systems lies in their importance in reactivity of biological systems. For instance, they serve as 'relay stations'[9] in ubiquitous electron transfers.[10,11] Special importance is given to disulfides, because of their essential role for structure and reactivity of proteins. These radical anions (noted 2S-3e) have thus been intensively studied, either on model organic compounds,[12−16] organometallic complexes,[17,18] and biological systems, in which they have been recognized as long-lifetime intermediates.[19,20]

One would like to gain insight into the factors governing the formation, the stability and the outcome of these transient 2S-3e intermediates in a complex environment. Recently enough, Weik and co-workers have nicely demonstrated using X-ray synchrotron radiations the high specificity of low-energy electrons addition,[21] with a valence attachment on low-lying σ^* (SS) orbitals. Quantum calculations, alongside with topological analysis,[22] offer a complementary view, often more quantitative, on the structure and reactivity of the 2S-3e intermediates. Many questions remain answerless

* Corresponding author e-mail: elise.dumont@ens-lyon.fr.
† UMR 5182 CNRS École Normale Supérieure de Lyon.
‡ Nancy-Université.
§ Present address: Research School of Chemistry, Australian National University, Canberra ACT 0200, Australia.

10.1021/ct900093h CCC: $40.75
Published on Web 04/30/2009

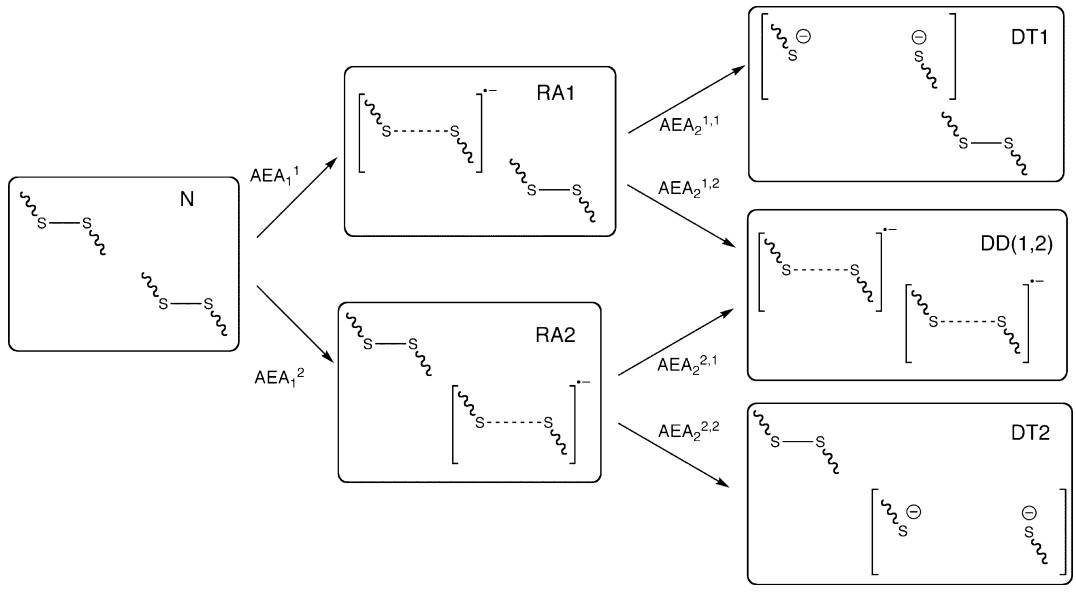

Figure 1. Schematic view of the possible outcomes of the stepwise two-electrons addition on a two-disulfide linked system. The square box represents the proteinic environment. The inner competition between the two disulfide bonds for the first electron uptake, with formation of radical anions (RA), is addressed by computing the respective adiabatic electron affinities AEA_1. Similarly, the addition of a second electron can form either a dithiolate (two possibilities DT1 or DT2) or a diradical dianion noted DD(1,2). Relative energies are computed to gain insights on such competitions.

concerning their formation, which is directly quantified by the electron affinity (EA). This intriguing reaction is formally simple and presents two key characteristics (cf. Figure 1): the drastic disulfide lengthening (by ca. 0.7 Å) and the charge difference between the reactant and the product. This gives rise to two major contributions, geometric and electrostatic, that both impact EA. Striking examples have been reported for the huge modulation by the following:

1. the conformational strain or topological frustration that strongly favors an electron uptake.[23−25] This purely geometric effect enhances EA by ca. 1 eV for a Cys-Gly-Pro-Cys motif (CGPC), which forms the active site of Trxh1, an antioxydant enzyme from the thioredoxin superfamily.
2. the secondary structure, for instance the effect of a α-helix dipole (+0.9 eV for an Ala_{12} grafted on CGPC, constituting a peptidomimetic for Trxh1),[26]
3. a point charge of +1 au even at a distance of 10 Å[27] or, more realistically, a charged residue in the vicinity of a disulfide (accounting for ca. 2.0 eV from the Lys40 residue of Trxh1).[28]

These simple considerations usually suffice to conclude on the relative reactivity of two highly similar disulfide bridges, e.g. to discuss mutation effects. Indeed, most of the available results so far have focused on Trx enzymes possessing a unique, highly reactive, disulfide linkage.[24,28] But several other questions naturally arise as a mutiply disulfide-linked protein is considered, e.g. *Torpedo Acetylcholine Esterase* (TAchE) in the original paper by Weik and co-workers.[21]

The first question concerns the relative order of reactivity of disulfides, with an inner competition to treat. Redox reactions do not involve a flow of electrons but rather one (or two), whose attachment is highly specific.

Other questions arise for the addition of a second electron. At first sight, the beautiful X-ray structure of irradiated *TAchE*, with each of its three disulfides in radical anionic form, may suggest that *n successive* electron additions on *n* disulfide linkages results in the formation of *n* radical anions. But the electron uptake could also occur on a 2S-3e bond, forming a dithiolate, especially in solution with no packing effects. Such a cleavage results in a fragmentation of the protein. Calculations provide a reliable way to gain some insights on the electronic pathway (inner competition, cf. Figure 1) for the second EA, while no information can be inferred from experimental data as *all* disulfide bridges are inevitably damaged under radiation process. For instance, quantum mechanics (QM) calculations on the isolated active site of *TAchE* prove the constrasted disulfide reactivity.[20]

In this study, we have undertaken a systematic study of two successive electron attachments on a small circular macropeptide, widely studied in the literature, kalata B1 (kB1). It is the prototype of the cyclotide family, small disulfide rich macropeptides isolated from plants. The three-dimensional structure (Figure 2) is well-defined with a cyclic backbone (Mobius type with a *cis* proline) and three interlocking disulfide linkages, forming a highly characteristic cystine knot motif. The latter not only maintains the circular compact folding (thermal stability) but also enhances disulfide reactivity because of the constrained topology. A whole line of research now consists in tuning in a controlled way infectiologic properties of cyclotides (HIV inhibitors,[29] antimicrobial).[30]

Some of the proper characteristics of cyclotides make them perfect candidates, in the context of this study, with several advantages over other systems, notably the following: three disulfides linkages at first sight rather similar, a circular structure that bypasses the need to cap the N- and C-terminal

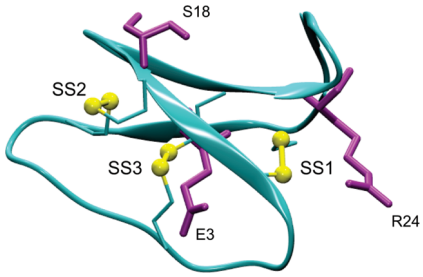

Figure 2. Cartoon representation of kalata B1 (PDB ID 1NB1). No proper secondary structure is defined because of the sequence short size and the cystine knot motif (interlocking arrangement of the three disulfide linkages Cys(1−15), Cys(10−22), and Cys(5−17) — labeled SS1, SS2, and SS3 on this scheme and represented with (yellow) balls). The latter imposes a tightly bent cyclic structure (backbone in cyan), with a Mobius topology (*cis* proline). Arginine R24, serine S18, and glutamate E3 side chains strongly tune disulfide electron affinities and are labeled and depicted with (purple) sticks.

residues, and, first and foremost, a wealth of experimental information.[31−34]

We built up in recent works[23,24,26] a methodology specifically tailored to accurately describe electron attachment on disulfide-linked systems, which is recalled in Section II. The selectivity of the first one-electron addition (inner competition) is analyzed with three different steps in Subsections 3.1, 3.2, and 3.3. The addition of a second electron is treated in the last Subsection (3.4); all possible adducts (nine) are considered to identify the electronically most stable product.

II. Computational Methodology: QM/MM Scheme

Due to the relatively large size of kB1 (29 residues, 376 atoms) and the high level of theory needed for describing electron attachment on disulfide bonds, hybrid Quantum Mechanics/Molecular Mechanics (QM/MM) methods offer a near-optimal approach. Moreover, they enable a decomposition of the overall EA into geometric and electrostatic contributions, as detailed in the last Subsection.

A. QM Description of 2S-3e Bond and Definitions of Relative AEAs. Explicit treatment of electron correlation is essential for an accurate description odd-electrons bonds. Second-order Møller−Plesset perturbation theory (MP2)[35] has proved its reliability for a proper description of 2S-3e bonds.[36,37] First adiabatic electronic affinities (AEA_1) of optimized structures were defined, as usual, as the difference between energies of the optimized reactant (neutral compound, N) and product (radical anion, RA):

$$AEA_1 = E(N) - E(RA) \quad (1)$$

AEAs have proved to be highly sensitive to the basis set,[38] which needs to be carefully calibrated to treat neutral and anionic species on the same footing. In contrast, relative values ΔAEA are stable as soon as the basis set includes diffuse functions on the sulfur atoms — one benefits from a cancelation of errors.[24,25] They were defined with respect to a L,L-cystine capped by acetyl and N-methylamide (cf. Figure 3), which we chose as a reference (cf. eq 2).

$$\Delta AEA = AEA_{kB1} - AEA_{L,L-cys} \quad (2)$$

In this study, we chose a mixed Pople basis set, with 6-31+G** on sulfur and 6-31G* for carbon and hydrogen atoms.

B. Two-Layers Partioning of a Disulfide-Linked Peptide: QM/MM Scheme and Classical MM Description. A double proximal C_α–C_β frontier is defined, isolating the -CH_2-S-S-CH_2- fragments of the three cystines (cf. Figure 3), within a hydrogen link-atom (HLA) scheme.[39,40] The scaling factor corresponding to the ratio between $R(C_\beta - HLA)$ and $R(C_\alpha - C_\beta)$ is fixed to 0.71.

The MM surrounding is described with the CHARMM force field using the CHARMM27 parameters for proteins.[41−43] The van der Waals parameters of the QM atoms are set to the values defined for the corresponding atom type of the force field. To avoid an overpolarization of the C_β-HLA bonds, the nearby C_α point charge, q_{C_α}, initially equal to 0.07 e, has been set to zero. The overall electroneutrality of the MM part is ensured by a redistribution on the nitrogen (−0.47 → −0.435 e) and carbon (0.51 → 0.545 e) neighboring atoms — cf. Figure 3. We checked on L,L-cystine and diethyldisulfide[26] that this operation does not impact relative electron affinities. The placement of a frontier along a covalent bond inevitably introduces an artifact. But, we have recently discussed the frontier effects on a model compound (diethyldisulfide)[24] and established the stability of relative energies with respect to the level of theory.

In this study, the high-level QM part corresponds to the union of the three -CH_2-S-S-CH_2- fragments, which defines a global wave function. Very similar geometric and energetic data for the additions of (i) one electron and of (ii) a second one on the same linkage (formation of a dithiolate) are obtained whether the QM part is limited to a single cystine

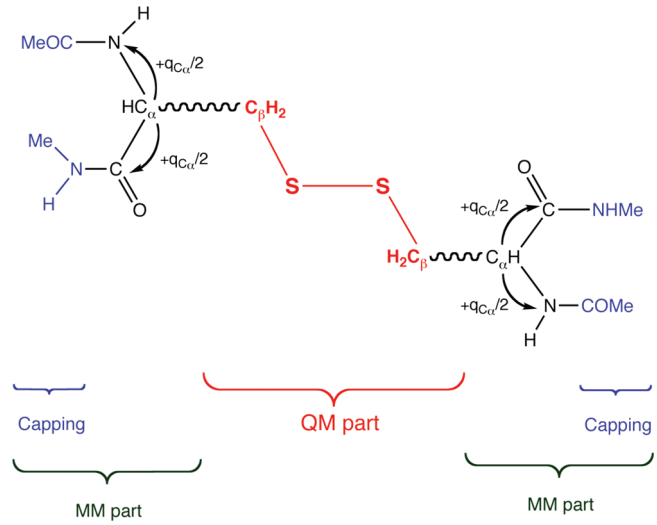

Figure 3. QM/MM partition adopted for describing electron addition on a disulfide linkage, illustrated on the capped L,L-cystine. This prototypical peptide constitutes the reference compound in this study. Wavy lines denote the C_α–C_β bonds which have been defined as QM/MM frontiers in this work. Atoms in bold (red) are treated with the MP2 method. Arrows indicate the charge redistribution ensuring the electroneutrality of the system. Terminal capping groups (NHMe and COMe) are indicated in blue.

Table 1. Geometrical Parameters (Respectively Bond Lengths, Bending and Dihedral Angles) and First Adiabatic Electron Affinities AEA_1 of kB1[a]

			structure				electron affinities			
linkage	label		*d*(S-S)	∠(S-S-C)	τ(C-S-S-C)	rmsd	AEA_1	ΔAEA_1	ΔEA_1^{elec}	ΔAEA_1^{geom}
Cys(1−15)	SS1	N	2.05	103.0, 106.0	95.5		1.58	0.52	0.78	−0.26
		RA	2.75	94.1, 106.8	132.5	0.87				
Cys(5−17)	SS2	N	2.06	102.8, 101.7	76.4		0.68	−0.38	0.31	−0.69
		RA	2.77	97.5, 91.7	70.3	0.23				
Cys(10−22)	SS3	N	2.06	101.3, 102.9	106.6		0.51	−0.55	0.24	−0.79
		RA	2.83	103.6, 104.4	81.7	0.28				
L,L-cystine	—	N	2.05	102.7, 104.7	75.2		1.06			
	—	RA	2.80	95.3, 95.8	66.5					

[a] The level of theory is detailled in the text. Absolute and relative values ΔAEA, with respect to L,L-cystine, are given in eV, for each of the three disulfide linkages. They are decomposed into electrostatic ΔAEA^{elec} and geometric ΔAEA^{geom} contributions. N or RA refer to neutral or radical anionic species. RMSD are reported for each RA with respect to the common neutral reference N.

or encompasses the three cystinyl fragments — cf. Table 2, Supporting Information, showing that having multiple QM/MM boundaries (six) does not induce any additional error.

Hybrid QM/MM calculations were performed with a modified version of the Gaussian 03 series of programs[44] linked to the Tinker software[45] for the MM calculations. Final geometrical parameters are given in angstroms (Å) and degrees. rmsd between neutral and (di)anionic forms were computed following the method of Kabsch[46] as implemented in the VMD software[47] — hydrogen atoms were excluded. The keyword guess = alter was used to force the initial SCF guess, thus obtaining each specific localized radical anions (RA), diradical dianions (DD), or dithiolates (DT). No spin contamination was observed for RA, with values of $\langle S^2 \rangle$ never greater than 0.77 (to be compared to the exact value of 0.75). DD can be found either in the triplet or the singlet states. For triplet states, $\langle S^2 \rangle$ values were never greater than 2.03 (to be compared to the exact values of 2.00), such that, again, no contamination spin will affect our results. The latter is observed for singlet states ($\langle S^2 \rangle$ up to 1.04) but does not affect the energetic results since singlet–triplet energy difference is negligeable (less than 1 kcal/mol, systematically in favor of the triplet state) was observed.

Cartesian coordinates for the NMR solution structure of kalata B1 were employed (PDB ID 1NB1). Each of the 20 experimental lowest energy geometries lead to the same 3D structure after classical optimization. Classical preoptimizations were performed using the minimize procedure of the TINKER suite of programs, with the lowest convergence criterion implemented — rms gradient of 0.1 kcal/mol/Å. All 20 NMR structures provide the same geometry of neutral kalata B1 (rmsd ranging between 0.257 and 0.332 with respect to PDB initial geometries). Starting from this structure of neutral kB1, QM/MM optimizations were performed for each electronic state (N, RA, DT, or DD): all residues (backbone and side chains) were varied, and the convergence was tested against standard criteria of Gaussian 03. For the neutral state, the MM and QM/MM optimized coordinate sets states give a rmsd of 1.311 (hydrogens excluded). We did not explore the existence of other possible minima. The existence of other local minima close in energy is unlikely because of the circular and very rigid structure of kB1. Only its side chains have some geometric freedom.

Amino acids are referred by the conventional one-letter code hereafter. The protonation state of the two charged amino acids (E3 and R24) was checked using propKa[48,49] (experimental conditions, pH = 6.1).

C. Decomposition into Electrostatic and Geometric Components. In our implementation, the QM wave function is polarized by the electric field created by MM point charges, which is referred to as electrostatic embedding (EE) hereafter. EE can be switched off by setting up all MM point charges to zero: corresponding values are noted $AEA^{\star}$. The two EE-free values, for kB1 and L,L-cystine, serve as calculus intermediates to decompose ΔAEA (eq 2) into geometric and electrostatic contributions. Such that, one can write

$$\begin{aligned}\Delta AEA &= AEA_{\mathrm{kB1}} - AEA_{\mathrm{L,L-cys}} \\ &= \underbrace{(AEA_{\mathrm{kB1}} - AEA^{\star}_{\mathrm{kB1}} - AEA_{\mathrm{L,L-cys}} + AEA^{\star}_{\mathrm{L,L-cys}})}_{\mathrm{elec}} + \\ &\quad \underbrace{AEA^{\star}_{\mathrm{kB1}} - AEA^{\star}_{\mathrm{L,L-cys}}}_{\mathrm{geom}} \\ &= \Delta AEA^{\mathrm{elec}} + \Delta AEA^{\mathrm{geom}}\end{aligned}$$

Rather intuitively, the mechanical constraint exerted by the protein on a cystine fragment corresponds to the difference between kB1 and the linear L,L-cystine, as all MM point charges are turned off. A residue-by-residue analysis of individual side-chain contributions to ΔAEA^{elec} is lead with exactly the same methodology. In contrast with the aforementioned global procedure, backbone point charges are not switched off to avoid the creation of an artificial dipole.[57]

III. Results and Discussion

Disulfide numerotation requires an arbitrary choice because of the circular structure of kB1. We followed the convention of Craik and co-workers, as indicated on Figure 2, with three linkages Cys(1−15), Cys(5−17), and Cys(10−22), where Cys denotes cystine. For the sake of conciseness, they are from now on single-number labeled (respectively SS1, SS2, and SS3) in that order.

A. Respective Reactivities for the One-Electron Addition. First adiabatic EA are reported in Table 1 for each disulfide bridge as well as geometric parameters for neutral and radical anionic forms. First of all, none of the three

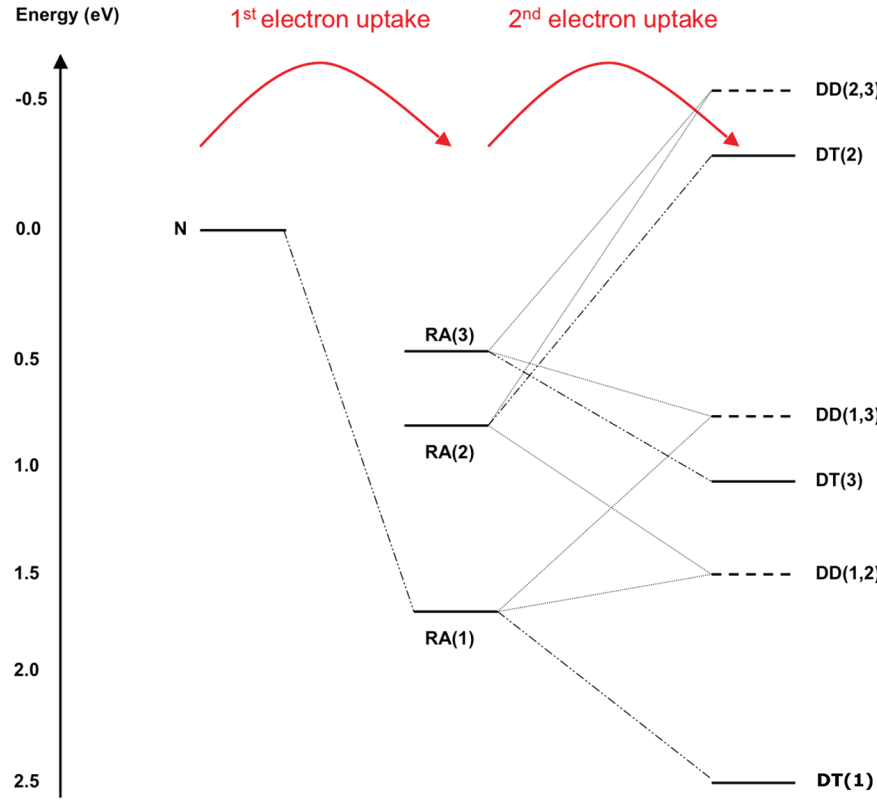

Figure 4. Relative energies (in eV) of kB1 products resulting from successive electron addition(s). RA denotes a (disulfide) radical anion, with the label of linked cysteines. DT (in solid line) refers to nonradical dianions (dithiolates) and DD (dashed lines) diradical dianions with two 2S-3e bonds. For the latter, singlet and triplet states have approximatively the same energies and thus do not appear separately. Corresponding numerical values are reported in Table 2. The neutral system (N) is taken as a reference of energy.

disulfide linkages is dissociated upon electron addition, which has to be noticed as a cleavage of the weak 2S-3e interaction can be observed in a highly dissymmetric environment.[50,51] Moreover, Mulliken spin densities (reported in Supporting Information, Table 1) are almost equally distributed on each sulfur center.

Values of ΔAEAs of +0.52, −0.38, and −0.55 eV are computed respectively for SS1, SS2, and SS3. SS1 is the most reactive toward electron uptake. One can note that Craik et al. proved experimentally that this linkage also exhibits the highest reactivity toward reducing alkylation.[33] We[24−26] and others[5] conjectured a possible analogy between disulfide electron affinity and redox potential. In contrast, the two other disulfide linkages are significantly less prone to capture an electron. How does the proteinic environment tune disulfide electron affinity, which is either increased or decreased with respect to L,L-cystine? To answer this question, ΔAEA are decomposed into electrostatic and geometrical contributions. Their values, gathered in Table 1, indicate that both effects importantly impact on AEA. They are examined in the next two subsections.

B. Residue-by-Residue Decomposition of the Electrostatic Component. The electrostatic modulation from the highly dissymmetric distribution of charge of the protein is an important factor orientating the inner competition for an electron uptake. It is intuitive that the presence of some charged residues in the vicinity of a neutral disulfide is decisive, as ascertained and quantified by previous studies. SS1 is indeed spatially the closest to an arginine, the 24th residue (R24), the sole positively charged residue of kB1 (Figure 2). Yet, its contribution may be counterbalanced by other residues (notably E3, the sole negatively charged one of kB1). Therefore, we performed a more systematic residue-by-residue analysis.

The individual side-chain contributions ΔAEA_l were computed, according to the procedure described in Subsection 2.3. They are monitored in Figure 5, as a function of a *m*-th residue whose side-chain electrostatic contribution is switched off. For comparative purposes, in the intermediate situation where all point charges of the side chain are turned off, but the backbone still polarizes the QM wave function, $AEA_l^{backbone}$, are rather similar (0.74, 0.98, and 0.71 eV, respectively). ΔAEA_l are reported in Table 3 of the Supporting Information as well as distances between disulfide barycenters and C_α positions of each constituting amino acid of kB1 on its optimized geometry. The following comments can be made:

1. As expected, R24 strongly enhances AEA, by 3.11, 1.29, and 1.05 eV for SS1, SS3, and SS2. These increments follow the distances between its C_α, and SS barycenters are 4.83, 8.03, and 10.57 Å, respectively.
2. Conversely, E3 disfavors an electron uptake by 1.76, 1.34, and 2.30 eV, respectively, for SS1, SS2, and SS3, distant by 7.11, 8.47, and 5.34 Å.
3. The decomposition picks out a third *neutral* residue, namely S18, with ΔAEA_l of 0.07, −0.35, and −0.16

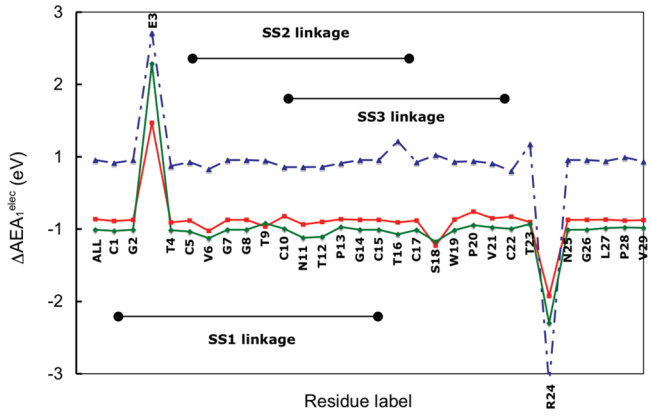

Figure 5. Variations of ΔAEA_1 for each of the three disulfide linkages of kB1, as a function of the residue number whose side chain partial charges are turned off. Values for the most reactive linkage SS1 correspond to the dashed line with (blue) triangles, with SS2 and SS3, respectively, correspond to the (red) square dots and (green) circles. In all cases, the two charged amino acids (E3, R24) exhibit important contributions, whose amplitude depends on their distance to the disulfide barycenter. The remaining of constituting residues of kB1 forms an apolar baseline.

for SS1, SS2, and SS3 linkages. This is most likely related to recent observations that serine, one of the most polar amino acid,[52,53] plays a specific role in tuning the redox potential of -Ser-Cys-Cys-Ser- (SCCS) motifs.[54]

4. In contrast, most of the remaining amino acids in the sequence of kB1 (glycine G, alanine A, valine V, leucine L, isoleucine I, proline P,... usually classified as neutral apolar) form an apolar baseline. They do not significantly impact on EA (variations lower than 0.04 eV in absolute values).

These results draw a simple conclusion, as do Coulomb laws: the closer the residue and the higher its polarity, the stronger its impact on electron affinity. Yet, this should not blur that even nonpolar residues also impact EA, more indirectly, by defining the secondary and tertiary structures. In turn, they create the backbone electrostatic field but also impose a mechanical constraint. The decomposition of ΔAEA_1 clearly denotes the importance of the geometrical effects that are analyzed in the next Subsection.

C. Geometrical Resistance to One-Electron Uptakes. The geometrical contribution ΔAEA^{geom} are quantified with respect to the linear L,L-cystine, for which no steric hindrance exists, and values for each disulfide are reported in the last column of Table 1. Generally speaking, its sign can be either

• positive if the disulfide elongation induced by the one-electron uptake is associated with a release of conformational strain, hence energetically favoring the anionic form. This is often the case of sequentially closed cysteines, like Trx.[24]

• or negative when the drastic disulfide lengthening is geometrically disfavored — for instance in a designed hairpin, with more separated cysteinyl residues.[24]

The negative signs computed for kB1 characterize an energetic penalty that systematically disfavors the anionic form. More quantitatively, SS1 differs from the two others disulfides solely from a geometrical point of view, with a purely mechanical energetic penalty on ΔAEA roughly halved (−8.3 vs −15.9 and −18.2 kcal/mol, values reported in eV in Table 1). This suggests that, as the compact Mobius structure is enforced, the SS1 elongation induces comparatively less defavorable structural changes.[58] The higher malleability of this linkage is further examplified by the variation of dihedral angle τ(C-S-S-C) by 37 degrees. rmsd provide a more global measure of the geometrical reorganization imposed by a disulfide lengthening: values are lower for SS2 and SS3 than for SS1 (respectively 0.23, 0.28, and 0.87 — values in Table 1). This lies in perfect agreement with experimental studies: Craik and co-workers proved that the Ala(1−15) mutant of kB1 conserves a very similar structure to the wild-type protein[32] and came to the conclusion that SS2 and SS3 define the structure of cyclotides, while SS1 is solely responsible for reactivity properties.[32]

D. Second Electron Uptake: A Competition between Dithiolates and Diradical Anions. We now discuss the addition of a second electron, with the competitive formation of a dithiolate or of a second disulfide radical anion (DT vs DD). Electronic energies of all nine possible dianions (three closed-shell dithiolates and six open-shell diradicals, either singlet or triplet) were computed to identify the most stable product. Data are reported in Table 2, and energy levels for neutral, anionic, and dianionic species are displayed on Figure 4. This diagram indicates, with no ambiguity, that the formation of the dithiolate SS1 is strongly favored over other possible adducts, with a spread of ca. 3 eV. The next paragraph explains how the proteinic environment of kB1 induces this orientation.[59]

The two main reasons why this contribution is neglected in this study are as follows: (i) a propKa calculation on the QM/MM optimized structure of DT1 indicating that no proton transfer occurs between the dithiolate DT1 and the R24 residue (whose pK_a is 11.24, to be compared to the reference pK_a of 12.50) and (ii) a large distance (5.60 Å) between the barycenter of S8—S167 and the barycenter of the N—N segment of R24 extremity. Also, whenever existing, such a charge transfer will in the first place stabilize DT1, the lowest energy structure (and the most prone to charge transfer).

Our results clearly show that the ease of reorganization of the protein upon disulfide elongation (by ca. 0.7 Å as a radical anion is formed, or by at least 2 Å for the formation of a dithiolate) is a decisive factor for the stabilization of a dianion. We first limit the discussion to dithiolates. DT1 is the most stable entity, by 1.38 and 2.72 eV over DT3 and DT2: the larger the distance between the two negatively charged sulfurs, the lower the energy. (Intersulfur distances, reported in Table 2 are respectively 6.68, 5.77, and 4.70 Å.) The local rigidity of the structural SS2 linkage prevents a spatial separation needed to stabilize the dianion. In contrast, a close inspection of the optimized geometry of the SS1 dithiolate (Figure 6c), compared to the structures of the neutral and anionic species (Figure 6a,b), reveals a different orientation of the R24 side chain. Its positively charged end $-CH(NH_2)_2^+$ points in the direction of the cleaved 1−15 disulfide and helps to stabilize one of the thiolates (C15). This motion is associated with the formation of a new

Table 2. Geometries, RMSD and Relative Energies (in eV) of Dianionic Forms of kB1 - Dithiolates (DT) or Diradical Dianions (DD)[a]

compounds			structure				
	2S+1	linkage(s)	d(S−S)	∠(S-S-C)	τ(C-S-S-C)	rmsd	energy ΔE
			Dithiolates				
DT1	1	SS1	6.68	70.9, 120.5	146.8	1.12	2.47
DT2	1	SS2	4.70	76.2, 83.1	78.2	0.57	−0.25
DT3	1	SS3	5.77	39.6, 109.3	114.2	1.44	1.09
			Diradical Dianions				
DD(1,2)	1	SS1	2.76	92.1, 99.3	128.8	0.83	0.88
		SS2	2.76	91.2, 96.4	68.8		
	3	SS1	2.76	92.1, 99.3	128.8	0.83	0.88
		SS2	2.76	91.2, 96.4	68.8		
DD(1,3)	1	SS1	4.97	81.7, 113.8	135.0	1.05	0.40
		SS3	2.75	98.1, 93.6	120.6		
	3	SS1	5.97	94.1, 106.0	120.2	1.51	0.40
		SS3	2.76	90.6, 90.6	125.3		
DD(2,3)	1	SS2	2.76	94.9, 92.4	62.3	0.64	−0.50
		SS3	2.71	50.3, 91.4	118.3		
	3	SS2	2.76	94.9, 92.4	62.3	0.64	−0.51
		SS3	2.72	94.2, 91.4	118.4		

[a] Mulliken spin densities are given in Table 1, Supporting Information. Relative energies ΔE are calculated with the neutral (N) compound taken as a reference — cf. Figure 4.

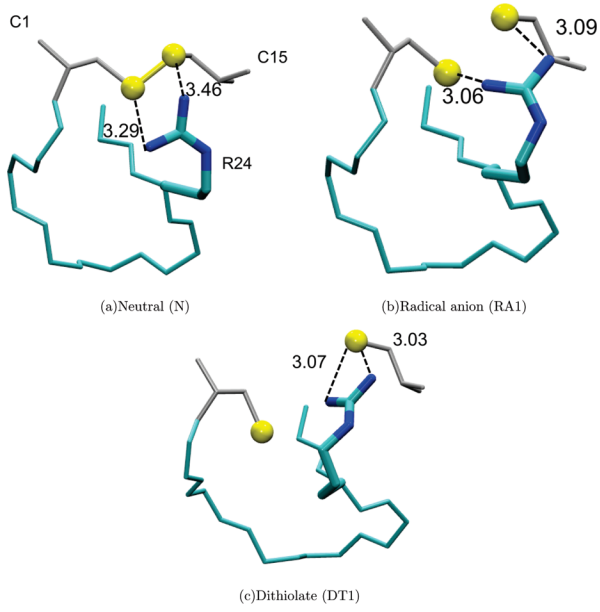

Figure 6. Partial view of kB1 optimized structures, centered on the SS1 linkage. The backbone is displayed with (green) light sticks, and arginine 24 side chain (R24), which plays a crucial role in tuning the one- and two-electron uptake, in bolder sticks. We report for each structure the two lower distances (in Å) between nitrogens of R24 and sulfurs of C1 and C15. A dissymmetry appears as the disulfide bond is disrupted (dithiolate DT1), and the side chain of R24 stabilizes the C15 sulfur thiolate.

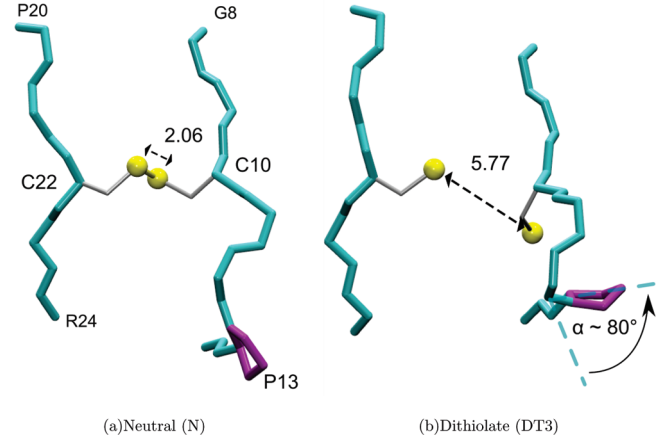

Figure 7. Optimized structures of kB1, in the neutral (left side) and dianionic (right side) forms, centered on the SS3 linkage. The backbone is depicted with (green) sticks, and the side chain of proline P13 with purple sticks, while the two sulfur atoms are displayed with (yellow) balls. Distances are reported in Å. One notes a large amplitude motion of the P13-G14 β-turn, with a characteristic angle α of ca. 80 degrees.

hydrogen bond network in the vicinity of R24. Both effects counterbalance the repulsion of the two negatively charged sulfur atoms. In between, DT3 is also stabilized by a flip of the P13-G14 β-turn upon the 3.71 Å elongation of the initially covalent SS — represented in Figure 7. This large amplitude motion (rmsd value of 1.51, characterized by an α angle of ca. 80 degrees) induces a flip of the -CH_2-S^- side chain of C10. Its sulfur atom rotates to point oppositely to the other C22 sulfur, whose position remains almost unchanged.

The most stable of the three diradical dianions, DD(1,2), could have been predicted from the reactivity order for the first electron uptake (AEA_1, cf. Figure 4). Most likely, the presence of E3 governs the energetic positions of DD(1,2) vs DD(1,3).

The latter compound examplifies an interesting structural outcome. The electron addition on the SS3 linkage induces a cleavage of the 2S-3e bond of the SS1 radical anion, with a distance passing from 2.75 to 4.97 Å. R24, initially equidistant to each sulfur of the SS1 linkage (Figure 6b), stabilizes one of the thiolates (C1) — the situation is close to Figure 6c. This evolution can be related to the charge-assisted electron capture dissocation of disulfide, studied by both experimental[55] and theoretical means.[50]

One should keep in mind that the formation of a dithiolate, even energetically favored, would probably not be observed if crystals of kB1 were irradiated, because the geometrical relaxation is hindered/prevented in a crystallic structure (packing effect). Our calculations provide a complementary

view on the competitive formation of one- and two-electron addition adducts.

IV. Concluding Remarks

In this work, we examplified on the prototypic cyclotide, kalata B1, how a proteinic environment can dramatically tune the one- and two-electron reactivity of disulfide linkages. The factors governing the inner competition for the valence-attachment or the formation of a dithiolate vs a second disulfide radical anion, concomitant to a partial unfolding, are traced back. *Both* the electrostatic field (largely dominated by the respective positions of R24, E3, and, in a lesser extent, S18) and the mechanical constraint intermingle to increase the electron affinity of one disulfide of the cystine knot motif for the one-electron addition. This decomposition may provide useful information for guiding experimental works aiming at understanding and ultimately tuning in a controlled way disulfide reactivity (systematic scanning mutagenesis on cyclotides).[56]

Comparison is made with experimental studies that also provide strong evidence for the reactive role of this linkage, in terms of redox potential. It is quite remarkable that the same factors seem to govern electron affinity or redox potential. This nascent similarity of behaviors deserves more systematic studies, in order to draw a parallel that might lead to a more unified view of disulfide reactivity.

Acknowledgment. This work was supported by computer resources of the University of Nancy I, France. The authors are grateful to Dr. Nicolas Ferré (Université Aix-Marseille I, France) for providing a local version of the link atom scheme. A.D.L. and X.A. also acknowledge financial support from the Jean Barriol Institute (FR CNRS 2843). One of us (P.F.L.) thanks the Australian Research Council (ARC) for a postdoctoral fellowship.

Supporting Information Available: Mulliken spin densities of the nine radical structures, structures and electron affinities of neutral, radical anions and dithiolates described with a single -CH_2-S-S-CH_2- QM part, and numerical data corresponding to Figure 5. This material is available free of charge via the Internet at http://pubs.acs.org.

References

(1) Pauling, L. *J. Am. Chem. Soc.* **1931**, *53*, 1367–1400.

(2) Gill, P. M. W.; Radom, L. *J. Am. Chem. Soc.* **1987**, *110*, 4931–4941.

(3) Asmus, K. D. *Acc. Chem. Res.* **1979**, *12*, 436–442.

(4) Tung, T.-L.; John Stone, A. *Can. J. Chem.* **1975**, *53*, 3153–3157.

(5) Houée-Levin, C.; Bergès, J. *Radiat. Phys. Chem.* **2008**, *77*, 1286–1289.

(6) Fang, X.; Wu, J.; Wei, G.; Schuchmann, H. P.; von Sonntag, C. *Int. J. Radiat. Biol.* **1995**, *68*, 459–466.

(7) Lawrence, C. C.; Bennati, M.; Obias, H. V.; Bar, G.; Griffin, R. G.; Stubbe, J. *Proc. Natl. Acad. Sci. U. S. A.* **1999**, *96*, 8979–8984.

(8) Johnson, D. L.; Polyak, S. W.; Wallace, J. C.; Martin, L. L. *Peptide Sci.* **2003**, *10*, 495–500.

(9) Chen, X.; Zhang, L.; Wang, Z.; Li, J.; Wang, W.; Bu, Y. *J. Phys. Chem. B* **2008**, *112*, 14302–14311.

(10) Lao, Y.-T.; Abu-Irhayem, E.; Kraatz, H.-B. *Chem.–Eur. J.* **2005**, *11*, 5186–5194.

(11) Glese, B.; Graber, M.; Cordes, M. *Curr. Opin. Chem. Biol.* 2008. asap.

(12) Gauduel, Y.; Gelabert, H.; Guilloud, F. *J. Am. Chem. Soc.* **2000**, *122* (21), 5082–5091.

(13) Gauduel, Y.; Marignier, J. L.; Belloni, J.; Gelabert, H. *J. Phys. Chem. A* **1997**, *101* (48), 8979–8986.

(14) Gauduel, Y.; Launay, T.; Hallou, A. *J. Phys. Chem. A* **2002**, *106*, 1727–1732.

(15) Antonello, S.; Benassi, R.; Gavioli, G.; Taddei, F.; Maran, F. *J. Am. Chem. Soc.* **2002**, *124*, 7529–7538.

(16) Antonello, S.; Daasbjerg, K.; Jensen, H.; Taddei, F.; Maran, F. *J. Am. Chem. Soc.* **2003**, *125*, 14905–14916.

(17) Wenska, G.; Filipiak, P.; Asmus, K.; Bobrowski, K.; Koput, J.; Marciniak, B. *J. Phys. Chem. B* **2008**, *112*, 10045–10053.

(18) Ya. Melńikov, M.; Weinstein, J. A. *High Energy Chem.* **2008**, *42*, 329–331.

(19) Carles, S.; Lecomte, F.; Schermann, J.-P.; Desfrancois, C.; Xu, S.; Milles, J. M.; Bowen, K. H.; Bergès, J.; Houée-Levin, C. *J. Phys. Chem. A* **2001**, *105*, 5622–5626.

(20) Weik, M.; Bergès, J.; Raves, M. L.; Gros, P.; McSweeney, S.; Silman, I.; Sussman, J. L.; Houée-Levin, C.; Ravelli, R. B. G. *J. Synchroton Radiat.* **2002**, *9*, 342–346.

(21) Weik, M.; Ravelli, R. B.; Silman, I.; Sussman, J. L.; Gros, P.; Kroon, J. *Proc. Natl. Acad. Sci. U. S. A.* **2000**, *97*, 623–628.

(22) Fourre, I.; Silvi, B. *Heteroat. Chem.* **2007**, *18*, 135–160.

(23) Dumont, E.; Loos, P.-F.; Assfeld, X. *Chem. Phys. Lett.* **2008**, *458*, 276–280.

(24) Dumont, E.; Loos, P.-F.; Assfeld, X. *J. Phys. Chem. B* **2008**, *112*, 13661–13669.

(25) Dumont, E.; Loos, P. F.; Laurent, A. D.; Assfeld, X. *Int. J. Quantum Chem.* 2009. in press.

(26) Dumont, E.; Loos, P.-F.; Laurent, A. D.; Assfeld, X. *J. Chem. Theory Comput.* **2008**, *4*, 1171–1173.

(27) Sawicka, A.; Berdys-Kochanska, J.; Skurski, P.; Simons, J. *Int. J. Quantum Chem.* **2005**, *102*, 838–846.

(28) Rickard, G. A.; Bergès, J.; Houée-Levin, C.; Rauk, A. *J. Phys. Chem. B* **2008**, *112*, 5774–5787.

(29) Ireland, D. C.; Wang, C. K.; Wilson, J. A.; Gustafson, K. R.; Craik, D. J. *Peptide Sci.* **2007**, *90*, 51–60.

(30) Shenkarev, Z. O.; Nadezhdin, K. D.; Sobol, V. A.; Sobol, A. G.; Skjeldal, L.; Arseniev, A. S. *FEBS* **2006**, *273*, 2658–2672.

(31) Colgrave, M. L.; Craik, D. J. *Biochemistry* **2004**, *43*, 5965–5975.

(32) Daly, N. L.; Clark, R. J.; Craik, D. J. *J. Biol. Chem.* **2003**, *8*, 6314–6322.

(33) Goransson, U.; Craik, D. J. *J. Biol. Chem.* **2003**, *48*, 48188–48196.

(34) Clark, R. J.; Daly, N. L.; Craik, D. J. *Biochem. J.* **2006**, *394*, 85–93.

(35) Møller, C.; Plesset, M. S. *Phys. Rev.* **1934**, *46*, 618–622.

(36) Braida, B.; Hiberty, P. C.; Savin, A. *J. Phys. Chem. A* **1998**, *102*, 7872–7877.

(37) Humbel, S.; Demachy, I.; Hiberty, P. C. *Chem. Phys. Lett.* **1995**, *247*, 126–134.

(38) Rienstra-Kiracofe, J. C.; Tschumper, G. S.; Schaefer, H. F., III.; Nand, S.; Ellison, G. B. *Chem. Rev.* **2002**, *102*, 231–282.

(39) Humbel, S.; Sieber, S.; Morokuma, K. *J. Chem. Phys.* **1996**, *105*, 1959–1967.

(40) Dapprich, S.; Komárino, I.; Byun, K. S.; Morokuma, K.; Frisch, M. J. *J. Mol. Struct. (THEOCHEM)* **1999**, *461*, 1–21.

(41) MacKerel, A. D., Jr.; Bashford, D.; Bellott, M.; Dunbrack, R. L., Jr.; Evanseck, J. D.; Field, M. J.; Fischer, S.; Gao, J.; Guo, H.; Ha, S.; Joseph-McCarthy, D.; Kuchnir, L.; Kuczera, K.; Lau, F. T. K.; Mattos, C.; Michnick, S.; Ngo, T.; Nguyen, D. T.; Prodhom, B., III.; Reiher, W. E.; Roux, B.; Schlenkrich, M.; Smith, J. C.; Stote, R.; Straub, J.; Watanabe, M.; Wiórkiewicz-Kuczera, J.; Yin, D.; Karplus, M. *J. Phys. Chem. B* **1998**, *102*, 3586–3616.

(42) Brooks, B. R.; Bruccoleri, R. E.; Olafson, D. J.; States, D. J.; Swaminathan, S.; Karplus, M. *J. Comput. Chem.* **1983**, *4*, 187–217.

(43) MacKerell, A. D., Jr.; Brooks, C. L., III.; Nilsson, L.; Roux, B.; Won, Y.; Karplus M. John Wiley & Sons: Chichester, 1998; Vol. 1of The Encyclopedia of Computational Chemistry; p 271.

(44) Frisch, M. J.; Trucks, G. W.; Schlegel, H. B.; Scuseria, G. E.; Robb, M. A.; Cheeseman, J. R.; Montgomery, J. A., Jr.; Vreven, T.; Kudin, K. N.; Burant, J. C.; Millam, J. M.; Iyengar, S. S.; Tomasi, J.; Barone, V.; Mennucci, B.; Cossi, M.; Scalmani, G.; Rega, N.; Petersson, G. A.; Nakatsuji, H.; Hada, M.; Ehara, M.; Toyota, K.; Fukuda, R.; Hasegawa, J.; Ishida, M.; Nakajima, T.; Honda, Y.; Kitao, O.; Nakai, H.; Klene, M.; Li, X.; Knox, J. E.; Hratchian, H. P.; Cross, J. B.; Adamo, C.; Jaramillo, J.; Gomperts, R.; Stratmann, R. E.; Yazyev, O.; Austin, A. J.; Cammi, R.; Pomelli, C.; Ochterski, J. W.; Ayala, P. Y.; Morokuma, K.; Voth, G. A.; Salvador, P.; Dannenberg, J. J.; Zakrzewski, V. G.; Dapprich, S.; Daniels, A. D.; Strain, M. C.; Farkas, O.; Malick, D. K.; Rabuck, A. D.; Raghavachari, K.; Foresman, J. B.; Ortiz, J. V.; Cui, Q.; Baboul, A. G.; Clifford, S.; Cioslowski, J.; Stefanov, B. B.; Liu, G.; Liashenko, A.; Piskorz, P.; Komaromi, I.; Martin, R. L.; Fox, D. J.; Keith, T.; Al-Laham, M. A.; Peng, C. Y.; Nanayakkara, A.; Challacombe, M.; Gill, P. M. W.; Johnson, B.; Chen, W.; Wong, M. W.; Gonzalez, C.; Pople, J. A. *Gaussian 03, Revision B.05*; Gaussian, Inc.: Wallingford, CT, 2004.

(45) Ponder, J. W. *Tinker, version 4.2*; Washington University: St. Louis, MO, 2004.

(46) Kabsch, W. *Acta Crystallogr., Sect. A: Found. Crystallogr.* **1978**, *A34*, 827–828.

(47) Humphrey, W.; Dalke, A.; Schulten, K. *J. Mol. Graphics* **1996**, *14*, 33–38.

(48) Li, H.; Robertson, A. D.; Jensen, J. H. *Proteins* **2005**, *61*, 704–721.

(49) Bas, D. C.; Rodgers, D. M.; Jensen, J. H. *Proteins* **2008**, *73*, 765–783.

(50) Sawicka, A.; Skurski, P.; Hudgins, R. R.; Simons, J. *J. Phys. Chem. B* **2004**, *107*, 13505–13511.

(51) Anusiewicz, I.; Berdys-Kochanska, J.; Simons, J. *J. Phys. Chem. A* **2005**, *109*, 5801–5813.

(52) Grantham, R. *Science* **1974**, *185*, 862–864.

(53) Zimmerman, J. M.; Eliomi, N.; Simha, R. *J. Theor. Biol.* **1968**, *21*, 170–201.

(54) Gromer, S.; Johansson, L.; Bauer, H.; Arscott, L. D.; Rauch, S.; Ballou, D. P.; Williams, C. H., Jr.; Heiner Schirmer, R.; Arner, E. S. J. *Proc. Natl. Acad. Sci. U.S.A.* **2003**, *100*, 9533–9538.

(55) Zubarev, R. A.; Kelleher, N. L.; McLafferty, F. W. *J. Am. Chem. Soc.* **1998**, *120*, 3265–3266.

(56) Simonsen, S. M.; Sando, L.; Rosengren, K. J.; Wang, C. K.; Colgrave, M. L.; Daly, N. L.; Craik, D. J. *J. Biol. Chem.* **2008**, *283*, 9805–9813.

(57) If the point charges of an *i* residue were switched to zero, an artificial dipole would be created by the backbone nitrogen of the *i*-1 residue and the carbon of the $i + 1$ residue — corresponding to charges of -0.21 and $+0.21$ a.u., at a distance of ca. 5.5 Å.

(58) NMR 1H chemical shifts of kB1 also indicate '*a less structured local conformation*'.[32]

(59) One of the main drawbacks of QM/MM methods is to break artificially the possibility of a charge transfer. Two types of charge transfer can be considered, through the frontier bonds between the QM and the MM parts and through space. The excess electron is placed in the well localized $\sigma^\star$ (SS) orbital, and hence the charge transfer through the frontier bond is expected to be very small. (A MP2/6-31+G** calculation on diethyldisulfide shows that the terminal methyl groups have their Mulliken charges changed by less than 0.004e upon electron capture). For the through space charge transfer, several processes can occur. The two main reasons why this contribution is neglected in this study are as follows: (i) a propKa[48,49] calculation on the QM/MM optimized structure of DT1 indicating that no proton transfer occurs between the dithiolate DT1 and the R24 residue (whose pKa is 11.24, to be compared to the reference pKa of 12.50) and (ii) a large distance (5.60 Å) between the barycenter of S_8—S_{167} and the barycenter of the N—N segment of R24 extremity. Finally, whenever existing, such a charge transfer will in the first place stabilize DT1, the lowest energy structure (and the most prone to charge transfer), and thus not affect our conclusions.

CT900093H